Effect of hydrogen charging on dislocation multiplication in pre-strained super duplex stainless steel

X.Z. Liang[1], M.F. Dodge[2], S. Kabra[3], J.F. Kelleher[3], T.L. Lee[3], H. B. Dong[1*]

1. Department of Engineering, University of Leicester, University Road, Leicester LE1 7RH, UK
2. TWI Ltd., Great Abington, Cambridge CB21 6AL, UK
3. ISIS Neutron Source, Science and Technology Facilities Council, Rutherford Appleton Laboratory, Harwell Oxford, Didcot OX11 0QX, UK

Abstract

The effect of hydrogen charging on dislocation multiplication in super duplex stainless steel was investigated. Steel samples were pre-strained and charged with hydrogen for 10 days. Dislocation density was then measured using neutron diffraction. It is found that dislocation density multiplies by about one order of magnitude in samples with less than 5% pre-strain, but remains the same level in samples with pre-strain level of 10% and above.

***Key words**: dislocation density, stainless steel, hydrogen embrittlement, neutron diffraction*

Super duplex stainless steel (SDSS) comprises approximately equal phase fractions of austenite (γ) and ferrite (δ) [1-4]. This microstructure combination delivers superior corrosion resistance and good mechanical properties [5]. In recent decades, SDSS has seen increasing usage in chemical transport and processing facilities, including onshore refineries and subsea oil and gas flowlines [3-8].

In the offshore environment, flowlines would corrode freely in the marine environment under cathodic protection. However, the application of cathodic protection is not a risk-free method for materials. It has been widely reported that the application of cathodic protection can trigger the evolution of atomic hydrogen by which the macroscopic mechanical behaviour of materials can be often adversely affected [9-12]. Thus materials premature failure can be facilitated by the solute hydrogen, which is known as hydrogen embrittlement [13, 14].

Understanding of hydrogen-dislocation interaction is significant to comprehend hydrogen embrittlement [15-20]. The effect of hydrogen on dislocation density has previously been reported. For example, using X-ray diffraction, Chen et al. [16] and Deutges et al. [17] showed that the presence of hydrogen can trigger dislocation multiplication in palladium. Barnoush et al. [18] also reported that slip lines can arise on austenite surfaces during hydrogen charging using atomic force microscopy. These studies have generally been limited to near-surface techniques, making it difficult to isolate the effect of dislocation-surface interactions [21, 22]. However, the penetration depth of neutrons up to several cm in most metals can simultaneously provide bulk mechanical and microstructural property information non-destructively [23-29]. In this study, time-of-flight (TOF) neutron diffraction has been applied, for the first time, to reveal the effect of hydrogen on dislocation density in bulk SDSS.

A piece of bulk material was extracted from a UNS S32760 flowline, the measured chemical composition of which (in weight percentage) is 0.032%C, 0.54%Si, 0.72%Mn, 0.019%P,

0.009%S, 25.1%Cr, 3.56%Mo, 7.0%Ni, 0.01%Al, 0.01%As, 0.080%Co, 0.820%Cu, 0.040%Nb, 0.005%Sn, 0.007%Ti, 0.050%V, 0.680%W, 0.270%N with balance as Fe. Solution heat treatment was performed at 1200°C for 1 hour with water quenching to finish. Tensile samples were machined with a gauge volume of 35×5×1.2 mm^3. Sample surfaces were ground with emery paper up to 1200 grit. Three different pre-strained samples were prepared by applying 5%, 10% and 15% plastic pre-strain with a tensile strain rate of 10^{-3} s^{-1}, while unstrained samples were used as reference for neutron diffraction. Hydrogen pre-charging was conducted using a cathodic charging cell: samples were connected to cathodic lead and immersed into 3.5 wt.% NaCl solution at 50°C, whilst platinum wire was used as the anode. Hydrogen charging was applied for 10 days with a 25±5 mA/cm^2 current density.

A dramatic difference is reported on hydrogen diffusivity in ferrite and austenite. Ferrite has an order of 10^{-11} m^2/s for diffusion coefficient while it is 10^{-15} to 10^{-16} m^2/s for austenite at room temperature [30-32]. In SDSS, a diffusion coefficient is reported between 10^{-14} m^2/s and 10^{-15} m^2/s at room temperature [32]. In this study, an elevated 50°C temperature environment can give a higher hydrogen diffusivity, which an approximately 5 times higher hydrogen diffusivity can be achieved [32]. Therefore, it can be assumed that the hydrogen diffusivity of these samples is between 5×10^{-15} m^2/s and 5×10^{-14} m^2/s in this 50°C hydrogen charging environment. To estimate the hydrogen distribution after hydrogen charging, a hydrogen concentration of 40 ppm is assumed at the sample surface whilst it is 2 ppm in the sample. Fick's second law (whose solution is detailed in reference [32]) is applied here to model the hydrogen distribution in the sample and the result is shown in Fig.1. According to the result, hydrogen has penetrated more than half of the sample thickness after 10 days hydrogen charging.

Time-of-flight neutron diffraction experiments were performed on the ENGIN-X neutron diffractometer, ISIS, UK [33]. Fig. 2 shows schematic diagram of the set-up. A 4×4×2 mm^3

instrumental gauge volume was used (2 mm in the normal direction of the sample), from which the diffracted neutrons were acquired.

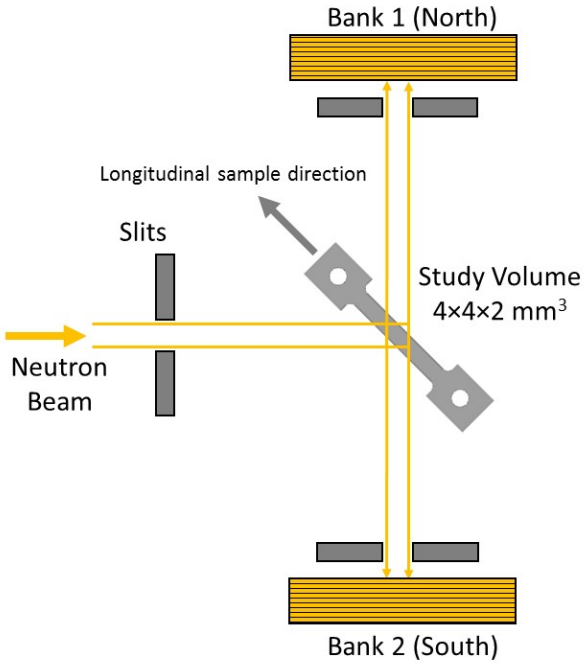

Figure 1 Schematic diagram of the neutron diffraction experiment setup on ENGIN-X instrument, at ISIS, Didcot, UK [33]

In 1955, Williamson et al. derived a model to calculate the dislocation density using X-ray spectrometry [34]. Based on this principle, in 2013, Christien et al. [26] proposed a dislocation density measurement method for neutron diffraction, which has been successfully applied to calculate dislocation density in a range of materials [35-37]. In 2015, Christien et al. [38] modified the materials elastic energy using the Faulkner equation (Eq. 3) to give a more accurate estimation compared with other experimental measurement methods. Here, we adopt this modification and briefly reorganize the derivation process.

The peak broadening Δd of neutron diffraction is related to interplanar d spacing, grain size t and elastic strain ε according to Williamson-Hall equation [39]:

$$\frac{\Delta d}{d} = \frac{d}{t} + \varepsilon \tag{1}$$

The peak broadening is usually determined by the increase of full width at half maximum (FWHM). In Eq. (1), the grain size term *d/t* contributes an approximately 10^{-5} for the overall peak broadening ratio *Δd/d* with an average grain size of tens of microns in SDSS as shown in Fig. 2. By comparison, the overall peak broadening ratio *Δd/d* is in the order of 10^{-3}, which is much larger than the grain size term *d/t* contribution. Therefore, the overall peak broadening *Δd/d* can be approximated by the elastic strain term *ε*:

$$\frac{\Delta d}{d} = \varepsilon \tag{2}$$

The total elastic energy *U* stored in the material can be calculated using the Faulkner equation [40]:

$$U = \frac{15}{4}\frac{E}{(1+v)}\varepsilon^2 = \frac{15}{4}\frac{E}{(1+v)}\left(\frac{\Delta d}{d}\right)^2 \tag{3}$$

where *E* is the Young's modulus and *v* is Poisson's ratio. The elastic energy per unit length of dislocation (*u*) can be estimated using the following equation for both edge and screw dislocations [41]:

$$u = \frac{Gb^2}{4\pi} ln \frac{r_1}{b} \tag{4}$$

where *G* is shear modulus, r_1 is the effective elastic field radius at a dislocation core and *b* is the burger's vector. We assume r_1=100 nm, *b*=0.248 nm for ferrite and *b*=0.254 nm for austenite. As the value $ln\frac{r_1}{b} \approx 2\pi$, the dislocation density can be derived from the Eq. (3) and (4), giving Eq. (5):

$$\rho = \frac{U}{u} = \frac{15E}{2Gb^2(1+v)}\left(\frac{\Delta d}{d}\right)^2 \tag{5}$$

Typical values of E/G=2.5 (G=200 GPa, E=80 GPa) and *v*=0.3 are used for both austenite and ferrite. To determine the peak broadening *Δd* value, the standard peak width reference was

obtained from the hydrogen free unstrained sample. An intrinsic 10^{12} m^{-2} dislocation density was assumed for the standard peak width.

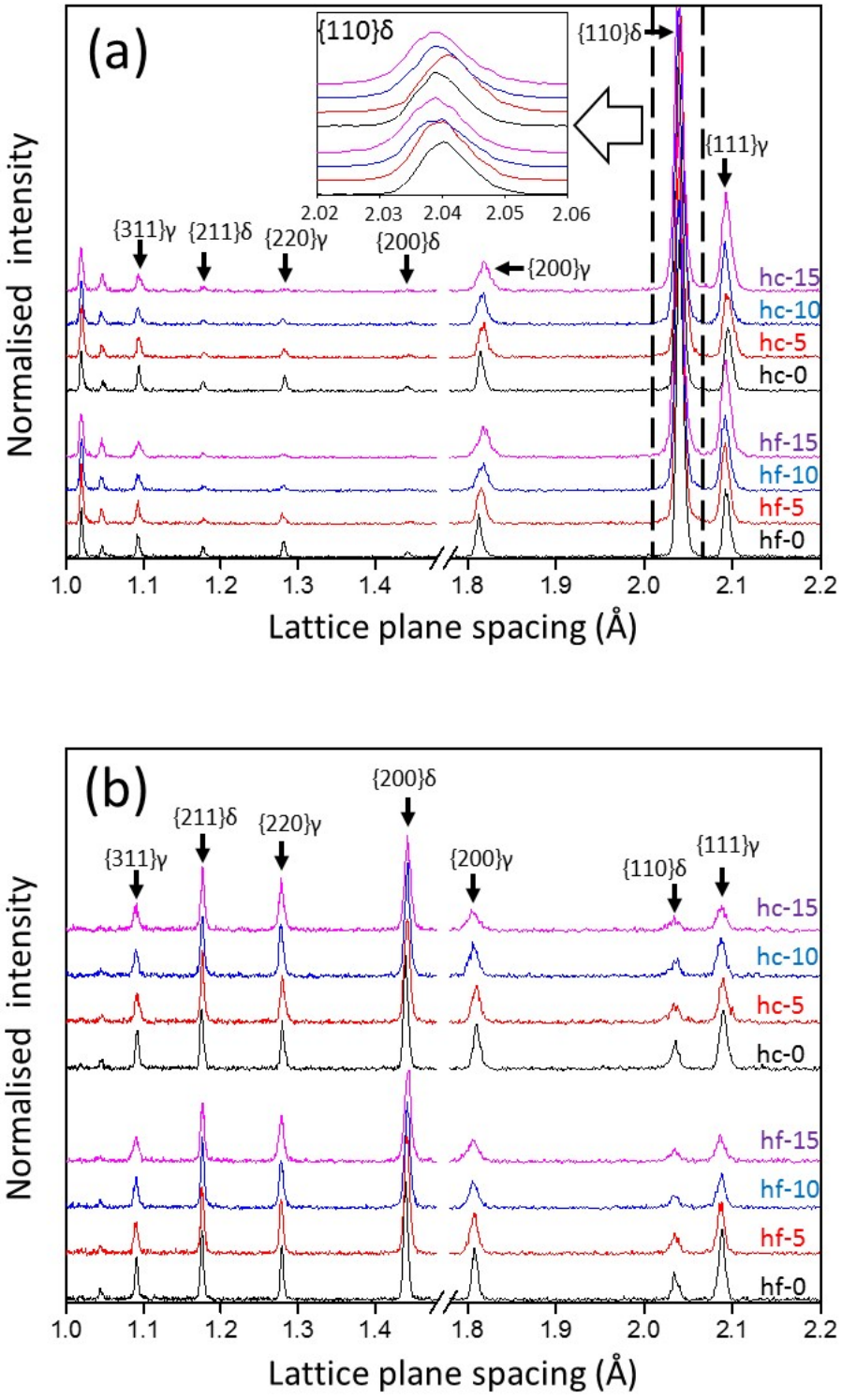

Figure 2 Neutron diffraction spectrum patterns of (a)lattice plane normal to sample longitude direction, signal collected from Bank 1; (b)lattice plane along sample longitude direction, signal collected from Bank 2. Abbreviations of hf and hc stand for hydrogen free and hydrogen charged, respectively. The numbers 0, 5, 10, and 15 represent the percentage of pre-strain.

Fig. 3 shows the TOF neutron diffraction spectrums collected from the North and South detector banks at ENGIN-X. North bank provides the neutron TOF data along the longitudinal direction of the sample, while South bank provides the data along the transverse direction. Along the longitudinal direction, the{111}γ and {110}δ peaks showed relatively higher peak intensity due to texture effect and therefore, these peaks were selected to determine the dislocation density. FWHM of each peak was determined from single-peak fitting method with a Voigt function using the OpenGENIE program [42]. Along the transverse direction of the sample, the δ dislocation density was determined by linearly averaging the dislocation density values derived from the {110}δ, {200}δ and {211}δ peaks, whereas the values from the{111}γ, {200}γ, {220}γ and {311}γ peaks were averaged to determine the γ dislocation density. The total dislocation density was then calculated by averaging the measured values of dislocation density from North bank and South bank.

Fig. 4 shows the dislocation density results for austenite and ferrite, with different pre-strain and hydrogen charge conditions. In the unstrained sample, an order of 10^{13} m^{-2} dislocation density was introduced into the austenite phase after hydrogen charging, whilst the dislocation density in ferrite increased, albeit to a lesser degree, realising a dislocation density of 5×10^{12} m^{-2}. A similar trend was revealed in the samples with 5% pre-strain. Such results suggest that solute hydrogen increases dislocation density for both austenite and ferrite. However, when 10% or 15% of pre-strain was applied, the hydrogen has nearly no effect on increasing dislocation density in both austenite and ferrite.

The stored dislocation density is a balance of athermal storage of dislocation and dynamic recovery [43]:

$$\frac{d_\rho}{d_\varepsilon} = \frac{d_{\rho^+}}{d\varepsilon} + \frac{d_{\rho^-}}{d\varepsilon} \tag{6}$$

where the term $d_{\rho^+}/d\varepsilon$ is dislocation generation and term $d_{\rho^-}/d\varepsilon$ is dislocation annihilation. In SDSS, the Frank-read-type source is suggested to account for dislocation density multiplication [18]. The critical shear stress required to activate the source is:

$$\tau = u\frac{2Gb}{l_d} \tag{7}$$

where G is the shear modulus, l_d is the segment length and u is the unit of dislocation line energy. An amount of residual stress always exists due to the property differences between the austenite and ferrite phases. In as-quenched SDSS, austenite has a tensile stress and ferrite has a compressive stress [44]. Kirchheim et al. [45, 46] suggested that the dislocation line energy can be reduced by the presence of solute hydrogen. Therefore, the critical shear stress required for the Frank-Read source is reduced, thus leading to dislocation multiplication.

However, the expended dislocation length by Frank-Read dislocation source multiplication is hindered in the samples with 10% and 15% pre-strain. As it has been mentioned above, a quenching process can introduce a residual stress between ferrite and austenite in SDSS [44]. This residual stress is critical for dislocation multiplication in samples without pre-strain and 5% pre-strain. However, in the samples with 10% and 15% pre-strain, a large scale plastic deformation is present. Johansson et al. [47] reported that, though ferrite undergoes more plastic deformation than austenite at low and intermediate macroscopic strain, the partitioning of plastic deformation from ferrite and austenite behaves indifferently at high macroscopic strains. Therefore, during the loading process, it can be proposed that the introduced plastic deformation can diminish the residual stress between the two phases from the as-quenched condition. Besides, as the mechanical properties of ferrite and austenite are close at the room temperature [47, 48], the release of loading can result in a low residual stress state in samples with 10% and 15% pre-strain. Consequently, the source of dislocation multiplication is reduced

and resulting in an equality of dislocation multiplication and annihilation in the samples with 10% and 15% pre-strain.

The model of dynamic recovery could be applied here to depict the dislocation evolution in these samples as hydrogen is able to activate the dislocation movement. Kocks and Mecking [49] proposed a systematic model to evaluate dislocation density within conditions of varying temperature and strain. Considering only the strain effect, the net storage rate of dislocation can be written as [49-51]:

$$\frac{d_\rho}{d_\varepsilon} = M(k_1\sqrt{\rho} - k_2\rho) \quad (8)$$

where M is Taylor's factor. k_1 is storage constant. k_2 is dynamic recovery constant which is proportional to the critical dislocation annihilation distance. Both k_1 and k_2 are positive values. As $k_2\rho$ possesses a higher order of term ρ than $k_1\sqrt{\rho}$, with increasing strain, the increase of dislocation density tends to slow down and finally achieve a dislocation saturated status. In the present study, hydrogen is shown to give rise to an increase in dislocation density in unstrained and 5% pre-strained samples, but not after the application of 10% and 15% pre-strain, which is likely due to this dislocation saturation phenomenon.

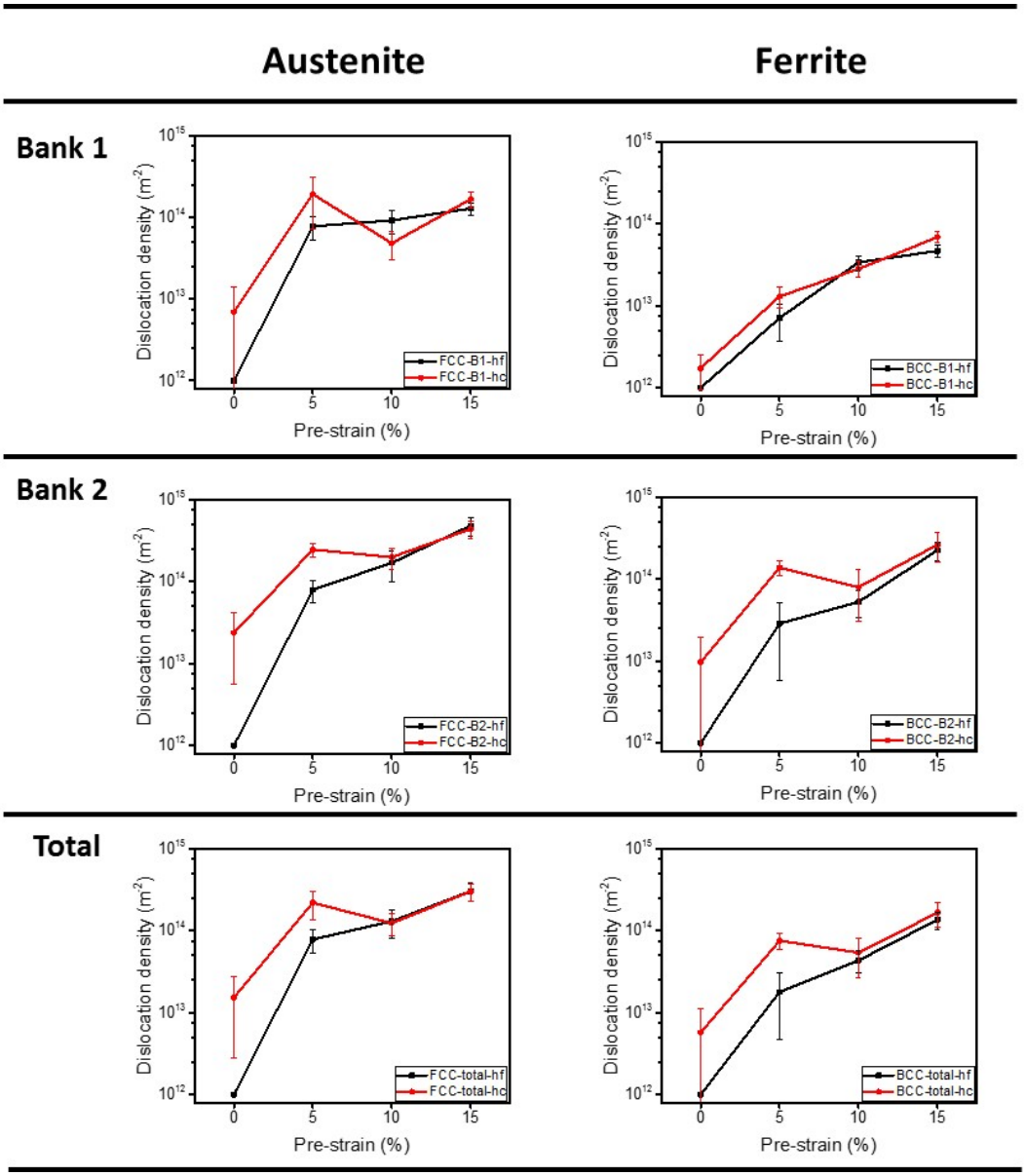

Figure 3 Dislocation density in austenite (FCC) and ferrite (BCC) as a function of different pre-strain; Bank1 reveals the dislocation density calculated from the lattice plane normal to sample longitude direction; Bank 2 depicts dislocation density calculated from the lattice plane normal to sample transverse direction; overall dislocation density is calculated by averaging the values of dislocation density determined from Bank 1 and Bank 2.

In summary, we reported hydrogen induced dislocation multiplication in super duplex stainless steel is a function of pre-strain, where multiplication of dislocation density manifests in samples with less than 5% pre-strain. Such dislocation multiplication is impeded when pre-strain reaches 10%.

Acknowledgement:

The authors acknowledge the allocation of beam time (RB1620333) at ISIS, Rutherford Appleton Laboratory, funded by the Science and Technology Facilities Council. TWI Ltd., Cambridge is gratefully acknowledged for supplying samples.

References

[1] H. Bhadeshia, R. Honeycombe, Steels Microstructure and Properties, Elsevier, Oxford, 2006.
[2] X.Z. Liang, M.F. Dodge, W. Liang, H.B. Dong, Scr. Mater., 127 (2017) 45-48.
[3] H.L. Yi, J.H. Ryu, H.K.D.H. Bhadeshia, H.W. Yen, J.R. Yang, Scr. Mater., 65 (2011) 604-607.
[4] T. Maki, T. Furuhara, K. Tsuzaki, ISIJ Int., 41 (2001) 571-579.
[5] T. Furuhara, T. Maki, J. Mater. Sci., 40 (2005) 919-926.
[6] I.N. Bastos, S.S.M. Tavares, F. Dalard, R.P. Nogueira, Scr. Mater., 57 (2007) 913-916.
[7] K. Devendranath Ramkumar, D. Mishra, B. Ganesh Raj, M.K. Vignesh, G. Thiruvengatam, S.P. Sudharshan, N. Arivazhagan, N. Sivashanmugam, A.M. Rabel, Mater. Design, 66, Part A (2015) 356-365.
[8] G. Lothongkum, P. Wongpanya, S. Morito, T. Furuhara, T. Maki, Corros. Sci., 48 (2006) 137-153.
[9] H.K.D.H. Bhadeshia, ISIJ Int., 56 (2016) 24-36.
[10] A. Elhoud, N. Renton, W. Deans, Int. J. of Hydrogen Energ., 35 (2010) 6455-6464.
[11] J. Song, W. Curtin, Nat. Mater., 12 (2013) 145-151.
[12] H.K.D.H. Bhadeshia, Prog. in Mater. Sci., 57 (2012) 268-435.
[13] A. Bahrami, P. Woollin, in: ASME 2010 29th International Conference on Ocean, Offshore and Arctic Engineering, American Society of Mechanical Engineers, 2010, pp. 13-22.
[14] A. Bahrami, A. Bourgeon, M. Cheaitani, in: ASME 2011 30th International Conference on Ocean, Offshore and Arctic Engineering, American Society of Mechanical Engineers, 2011, pp. 93-103.
[15] D.K. Han, Y.M. Kim, H.N. Han, H.K.D.H. Bhadeshia, D.-W. Suh, Scr. Mater., 80 (2014) 9-12.
[16] Y.Z. Chen, H.P. Barth, M. Deutges, C. Borchers, F. Liu, R. Kirchheim, Scr. Mater., 68 (2013) 743-746.
[17] M. Deutges, H.P. Barth, Y. Chen, C. Borchers, R. Kirchheim, Acta Mater., 82 (2015) 266-274.
[18] A. Barnoush, M. Zamanzade, H. Vehoff, Scr. Mater., 62 (2010) 242-245.
[19] A. Barnoush, C. Bies, H. Vehoff, Journal of Materials Research, 24 (2009) 1105-1113.
[20] A. Barnoush, H. Vehoff, Acta Mater., 58 (2010) 5274-5285.
[21] N. D'Souza, R. Beanland, C. Hayward, H.B. Dong, Acta Mater., 59 (2011) 1003-1013.
[22] G.K.H. Pang, K.Z. Baba-Kishi, A. Patel, Ultramicroscopy, 81 (2000) 35-40.
[23] M.F. Dodge, M.F. Gittos, H. Dong, S.Y. Zhang, S. Kabra, J.F. Kelleher, Mat. Sci. Eng. A, 627 (2015) 161-170.
[24] B. Abbey, S.Y. Zhang, M. Xie, X. Song, A.M. Korsunsky, Int. J. Mat. Res., 103 (2012) 234-241.
[25] S. Van Petegem, J. Wagner, T. Panzner, M.V. Upadhyay, T.T.T. Trang, H. Van Swygenhoven, Acta Mater., 105 (2016) 404-416.
[26] F. Christien, M.T.F. Telling, K.S. Knight, Scr. Mater., 68 (2013) 506-509.
[27] B. Abbey, S.Y. Zhang, W.J. Vorster, A.M. Korsunsky, Procedia Engineer., 1 (2009) 185-188.
[28] D.M. Collins, N. D'Souza, C. Panwisawas, Scr. Mater., 131 (2017) 103-107.
[29] T.L. Lee, J. Mi, S.L. Zhao, J.F. Fan, S.Y. Zhang, S. Kabra, P.S. Grant, Scr. Mater., 100 (2015) 82-85.
[30] E. Owczarek, T. Zakroczymski, Acta Mater., 48 (2000) 3059-3070.
[31] V. Olden, A. Saai, L. Jemblie, R. Johnsen, Int. J. Hydrogen Energy, 39 (2014) 1156-1163.
[32] V. Olden, C. Thaulow, R. Johnsen, Mater. Design, 29 (2008) 1934-1948.
[33] M. Daymond, L. Edwards, Neutron News, 15 (2004) 24-29.

[34] G.K. Williamson, R.E. Smallman, Philos. Mag., 1 (1956) 34-46.
[35] E.I. Galindo-Nava, P.E.J. Rivera-Díaz-del-Castillo, Acta Mater., 98 (2015) 81-93.
[36] B. Kim, E. Boucard, T. Sourmail, D. San Martín, N. Gey, P.E.J. Rivera-Díaz-del-Castillo, Acta Mater., 68 (2014) 169-178.
[37] M. Shamma, E.a.N. Caspi, B. Anasori, B. Clausen, D.W. Brown, S.C. Vogel, V. Presser, S. Amini, O. Yeheskel, M.W. Barsoum, Acta Mater., 98 (2015) 51-63.
[38] F. Christien, M.T.F. Telling, K.S. Knight, R. Le Gall, Rev. Sci. Instrum., 86 (2015) 053901.
[39] G.K. Williamson, W.H. Hall, Acta Metall., 1 (1953) 22-31.
[40] E.A. Faulkner, Philos. Mag., 5 (1960) 519-521.
[41] G.E. Dieter, D.J. Bacon, Mechanical metallurgy, McGraw-Hill New York, 1986.
[42] C. Moreton-Smith, S. Johnston, F. Akeroyd, J. Neutron Res., 4 (1996) 41-47.
[43] E. Nes, K. Marthinsen, Y. Brechet, Scr. Mater., 47 (2002) 607-611.
[44] S. Harjo, Y. Tomota, M. Ono, Acta Mater., 47 (1998) 353-362.
[45] R. Kirchheim, Acta Mater., 55 (2007) 5139-5148.
[46] A. Pundt, R. Kirchheim, Annu. Rev. Mater. Res., 36 (2006) 555-608.
[47] J. Johansson, M. Odén, X.-H. Zeng, Acta Mater., 47 (1999) 2669-2684.
[48] N. Jia, R. Lin Peng, Y. Wang, S. Johansson, P. Liaw, Acta Mater., 56 (2008) 782-793.
[49] U.F. Kocks, H. Mecking, Prog. Mater. Sci., 48 (2003) 171-273.
[50] M. Delincé, Y. Bréchet, J.D. Embury, M.G.D. Geers, P.J. Jacques, T. Pardoen, Acta Mater., 55 (2007) 2337-2350.
[51] B. Devincre, T. Hoc, L. Kubin, Science, 320 (2008) 1745-1748.